RESEARCH PAPER

Effect of patchwise slip on fluid flow

Maria Pihl · Bengt Jönsson · Marie Skepö

Abstract In this paper, we show that large *connected slip patches* (hydrophobic patches) are a necessity to induce macroscopic slip effects of water flow in microchannels. For this purpose, the 2D fluid flow between a planar stationary surface with alternating stick and slip patches and a parallel planar surface moving with a constant relative velocity has been studied by computer simulations based on Navier–Stokes equations. A *slip patch* is defined as the slipping length in a 2D system or a slip area of the surface in a 3D system. The simulations reveal that the ratio (size of each slip patch)/(distance between the two parallel interfaces) has profound effect on the viscous stress on the moving surface when this ratio is around and above one. However, when the ratio is much below one, the effect of the slip patches are minor, even if the area fraction of slip patches are higher than 50 %. Obviously, the stick patches adjacent to the slip patches act as effective barriers, preventing the fluid velocity to increase near the surface with alternating stick and slip patches. The obtained results are scalable and applicable on all length scales, with an exception for narrow channels in the subnano regime, i.e. <1 nm where specific effects as the atomistic composition and the nanostructure of the wall as well as the interactions between the wall and the water molecules have an effect.

M. Pihl
Applied Surface Chemistry, SuMo Biomaterials,
Chalmers University of Technology, Göteborg, Sweden

B. Jönsson
Biophysical Chemistry, Lund University, Lund, Sweden

M. Skepö (✉)
Theoretical Chemistry, Lund University, Lund, Sweden
e-mail: marie.skepo@teokem.lu.se

1 Introduction

There is an increasing interest in fluid flow in small, confined systems, i.e. microfluidics. This is partly due to new available methods of producing flow systems in the nano- and micrometre length scales, the importance of small volume handling in biology and biotechnology research, and the potential use of microfluidics in fundamental studies in biology and chemistry (Whitesides 2006). The microfluidic systems require the same components as a large-scale fluid system such as pumps, valves, and mixers, but since laminar flow dominates, driving and mixing of the fluids are difficult (Whitesides and Stroock 2001). However, there are different possible parameters to use for manipulating the fluid, for example, pressure, capillary effects, electric fields, magnetic fields, centrifugal forces, and acoustics, in addition to geometrical parameters (Stone et al. 2004).
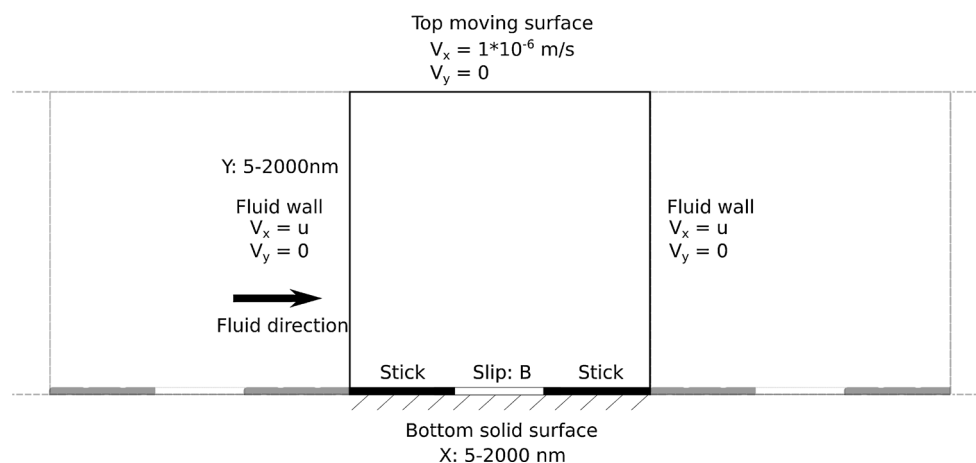
Another interesting parameter for fluid flow manipulation in systems on these length scales is slip. Slip is the presence of a tangential slip velocity (u_s) at a solid surface, proportional to the shear stress normal to the surface and may depend on several factors such as surface roughness, the presence of nanobubbles on the surface, wettability, and the solvent used (Tretheway and Meinhart 2004; Pit et al. 2000; Tyrrell and Attard 2001). By combination of surface chemistry and micropatering, superhydrophobic surfaces can be engineered. The surface structure alters the drops ability to stick and allow them to move very fast, one part of which is due to slip (David 2005). In water systems, hydrophilic surfaces show almost no slip whereas slip

Fig. 1 A schematic picture of the model system used in fluid flow computer simulations. The simulated system is periodic where each period has the length *X* and height *Y*. The model used had one *solid bottom* surface and one *upper* surface moving with a constant relative speed

Top moving surface
$V_x = 1*10^{-6}$ m/s
$V_y = 0$

Y: 5-2000nm
Fluid wall
$V_x = u$
$V_y = 0$

Fluid direction

Fluid wall
$V_x = u$
$V_y = 0$

Stick   Slip: B   Stick

Bottom solid surface
X: 5-2000 nm

lengths of a few tens of nanometres to some micrometre have been reported for hydrophobic surfaces (Bouzigues et al. 2008; Tretheway and Meinhart 2002; Brigo et al. 2008; Choi et al. 2003), and slip lengths up to 400 μm have been obtained for superhydrophobic surfaces (Lee and Kim 2009).

The aim of this study was to show that large *connected slip patches* (hydrophobic patches) are a necessity to induce macroscopic slip effects of water flow in microchannels. For this purpose, computer simulations with a 2D box model system in the nanometre range have been used. The effect of size and number of slip patches on the bulk flow has been investigated. We would like to emphasize that the study is directed into effective slip effects and bulk velocities, i.e. in the regime where Navier–Stokes equation of fluid flow is valid. For nanochannels with a width <10 nm, the atomistic composition and the structure of the wall as well as the interactions between the water and the walls influence the flow and the model is not applicable.

2 Model and methods

2.1 Model

To investigate the effect of slip on bulk fluid flow, a 2D box of width *X* and height *Y* (distance between bottom and upper surface) was created (see Fig. 1), and used in fluid flow simulations. The system consisted of one solid bottom surface and one upper moving surface. The solid surface was assumed to be the bottom surface of a larger microchannel, and the simulated fluid is water. The velocity in the *y* direction was set to zero and the fluid velocity in *x* direction was set to *u* for the two liquid walls. The upper surface was moving with the speed of 1×10^{-6} m/s. After the simulations were performed, the viscous force on the top moving surface was determined. The reference system was set to 100×100 nm, but both sides *X* and *Y* were

varied between 5 and 2,000 nm. The slip patch *B*, 0.1–99.9 % of the length of side *X*, was centrally positioned at the bottom surface *X* with adjacent no slip patches. The fluid flow was moving across the slip patches and the model was considered to be a part of a larger periodic system with the model system being the smallest part. In addition, a second model system was used where the stick and slip patches were reversed, i.e. one centrally placed stick region was placed in-between two slip regions, and a third model system consisting of 1–10 slip patches symmetrically placed on *X* adjacent to no slip patches was also created, with all other parameters kept as the first model.

The first model was used to study the effect of slip on fluid flow when altering the width and height of *X* and *Y*, and the third model were used to study the effect of slip on fluid flow with alternating slip and stick patches (no slip). The second model was only used to verify the resolution of the mesh size.

2.2 Computer simulations

Computer simulations of slip and fluid flow were performed in the COMSOL Multiphysics 4.3 software, using the microfluidics module (COMSOL AB, Stockholm, Sweden). This programme utilizes a finite element method to solve the Navier–Stokes equations, which in general form can be written:

$$\frac{\partial \rho}{\partial t} + \nabla(\rho \boldsymbol{u}) = 0 \qquad (1)$$

$$\rho \frac{\partial \boldsymbol{u}}{\partial t} + \rho (\boldsymbol{u} \cdot \nabla)\boldsymbol{u} = \nabla \cdot [-p\boldsymbol{I} + \tau] + \boldsymbol{F} \qquad (2)$$

where ρ is the density, $\boldsymbol{u}$ is the velocity, p is the pressure, τ is the viscous stress, $\boldsymbol{F}$ is the body forces, and $\boldsymbol{I}$ represents the 3×3 identity matrix. Equation 1 represents the conservation of mass and Eq. 2 represents the conservation of momentum. For all simulations, isothermal, stationary, laminar flow of an incompressible
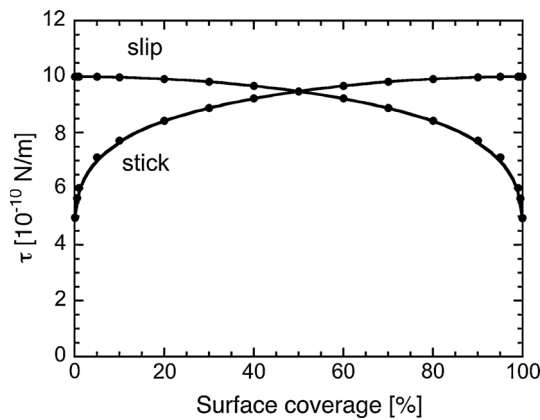
Fig. 2 The x component of the viscous stress for the reference systems ($X = Y = 100$ nm) as a function of surface coverage, where either stick or slip is simulated. The crossover at 50 % verifies the resolution of the simulations. *Marked circles* correspond to the calculated values, and the *line* is a guide for the eye
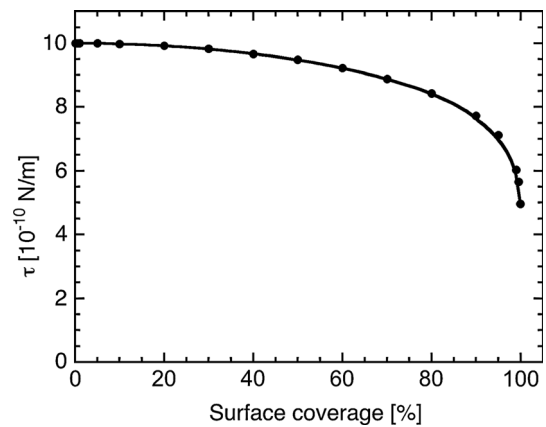

Fig. 3 Viscous stress as a function of slip surface coverage for the reference system of model 1. *Marked circles* correspond to simulated values, and the *line* is a guide for the eye. As the slip proportion of the width X increases, the viscous force on the top surface decreases

fluid (water) was assumed, and the Navier–Stokes equations governing the simulations can be simplified to:

$$\rho \nabla \cdot \boldsymbol{u} = 0 \tag{3}$$

$$\rho(\boldsymbol{u} \cdot \nabla)\boldsymbol{u} = \nabla \cdot \left[-p\boldsymbol{I} + \mu\left(\nabla \boldsymbol{u} + (\nabla \boldsymbol{u})^{\mathrm{T}}\right) \right] + \boldsymbol{F} \tag{4}$$

where μ is the dynamic viscosity. The slip boundary condition assumes that the fluid cannot penetrate the surface and that there is no viscous stress at the surface, i.e. no boundary layer, and that the slip length β is infinite. This can be expressed mathematically as:

$$\boldsymbol{u} \cdot \boldsymbol{n} = 0 \tag{5}$$

$$\left(-p\boldsymbol{I} + \mu\left(\nabla \boldsymbol{u} + (\nabla \boldsymbol{u})^{\mathrm{T}}\right) \right)\boldsymbol{n} = 0. \tag{6}$$

To verify the model system and achieve mesh independency, model 1 was meshed with gradually increasing mesh densities until obtained viscous stress converged. To further verify the resolution of the calculations, both model 1 and model 2 were used, with centrally placed slip or stick regions. The model reference system was of size 100×100 nm and the stick or slip patches were altered to constitute 0.1–99.9 % of the width X. Figure 2 shows the x-component of the viscous stress (τ) for the reference systems of the two models as a function of surface coverage where either stick or slip is simulated. The crossover at 50 % verifies the resolution of the simulations.

3 Results and discussion

The model 1 reference system of 100×100 nm was investigated, and the viscous force on the top moving

surface was determined while varying the slip patch size from 0.1 to 99.9 % of X. The concept of slip patch, a slipping length, or area of a surface is more intuitive than the parameter slip length, which is equal to the length inside the surface to which the fluid velocity is extrapolated to zero. In this study, we introduce the concept of slip patches and their influence on fluid flow, also the fraction of slip of a surface on fluid velocity is evaluated. Figure 3 shows the viscous stress τ as a function of surface slip fraction, where marked circles correspond to simulated values and the line is a guide for the eye. It is clearly visible that a larger slip patch induces a lower viscous force, i.e. a faster fluid velocity. For a more pronounced effect of slip on fluid velocity, the slip patch should be approximately 90 % of the total width.

In experimental settings, a striped surface with slip and no-slip regions could be obtained by altering superhydrophobic and hydrophilic patches. The superhydrophobic patches have the ability to trap gas, over which water can slip, whereas essentially no slip is detected for water passing over a hydrophilic surface (Bazant and Vinogradova 2008). There are several models describing fluid flow over striped patterns, both longitudinal and transverse to the fluid flow (Bazant and Vinogradova 2008; Zhou et al. 2012; Wang 2003; Stroock et al. 2002). In thin 3D channels, the striped patterns can cause a fluid flow transverse to the applied pressure gradient, which may be of potential use for microfluidic mixing (Feuillebois et al. 2010). In this type of application the transverse flow rates are maximized by using a rather large fraction ($\phi = 0.5$) of solid obstacles in the flow channel (Feuillebois et al. 2010).

The introduction of the hydrophobic patch gives rise to an increased velocity at the boundary and Fig. 4 shows the obtained excess velocity when a slip patch of 40 % (to the
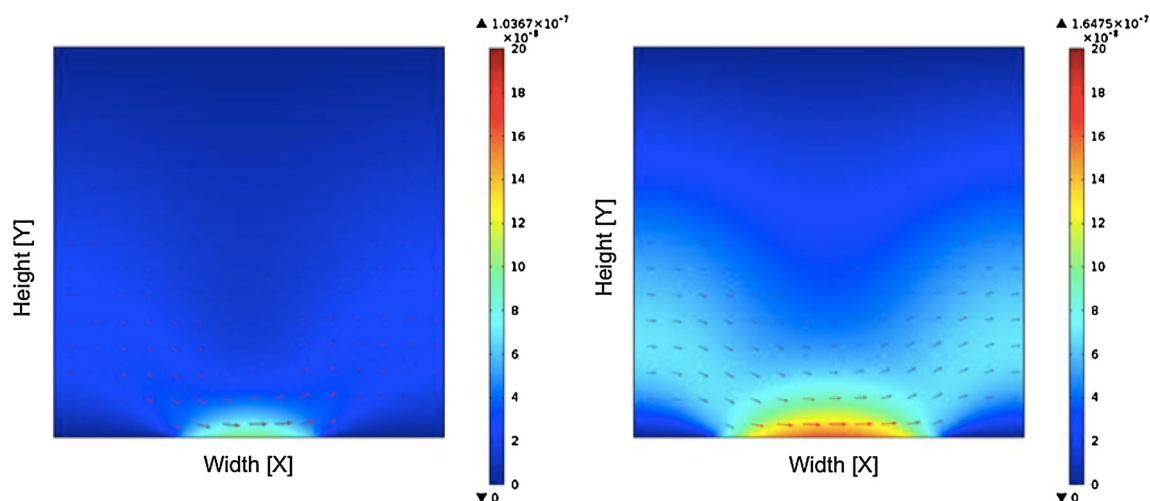
Fig. 4 Excess flow velocity profiles where a slip patch of 40 % (to the *left*) and 60 % (to the *right*) were implemented in the 2D model. Notice that: (1) the effect in Y direction is of the same size as the hydrophobic patch, and (2) the excess velocity is markedly affected by the size of the slip patch. Maximum obtained excess velocity is 1.0367×10^{-7} m/s in the flow profile to the *left* and 1.6475×10^{-7} m/s in the profile to the *right*, i.e. and increase of ≈ 60 %

left) and 60 % (to the right) are implemented in the model. It is clearly shown that a larger slip patch affects the fluid velocity more compared to a smaller slip patch and note that the size in Y direction that gives rise to the largest excess velocity is of the same size as the lateral distribution of the hydrophobic patch. Also the maximal excess velocity is increasing when the size of the slip patch is increasing cf. 1.0367×10^{-7} and 1.6475×10^{-7} m/s for 40 and 60 % slip, respectively, which corresponds to an increase of approximately 60 %. Interestingly, the stick patches adjacent to the slip patches act as barriers and prevent the fluid from gaining speed close to the wall. Note that the fluid velocity further out from the stick patch has an increased velocity due to the slip patch. In this study, we have simulated perfect slip, which is not possible to obtain in experimental settings where only a large effective slip can be obtained. Effective slip may be the result of surface heterogeneities, as a rough surface may hold gas pockets that can introduce slip (Lauga and Stone 2003), but it can also be true for smooth surfaces, where nanobubbles may be formed (Tyrrell and Attard 2001; Ishida et al. 2000). For superhydrophobic materials, slip lengths as large as 400 μm have been achieved (Lee and Kim 2009).

To further investigate the fluid behaviour in the presence of slip, model system 1 was used, and the height Y was varied between 100 and 800 nm. The width X was kept constant but its proportion of slip was varied between 0.1 and 99.9 %. Figure 5 shows the viscous force on the top moving surface as a function of slip surface coverage. When increasing Y, the viscous force on the top surface decreases. If the reference length Y is increased eight times, the viscous force for small slip patches (0.1 % of X) decreased from 10×10^{-10} to 1.25×10^{-10} N/m, i.e. a

decrease of almost 90 %, whereas for larger slip patches (99.9 % of X) the viscous force decreased from 5.0×10^{-10} to 1.1×10^{-10} N/m, or 80 %.

These results further demonstrate the small lengths scales at which slip operate. The ratio of the size of the slip patch, B, divided by the distance between the two parallel interfaces, Y shows that profound effects on the viscous stress are apparent when B/Y is around and above one (see Fig. 6).

Similar set-up was applied for studying the effect of X, where X was varied between 100 and 800 nm, the slip patch B between 0.1 and 99.9 %, and the height Y was kept constant and equal to 100 nm. The viscous force on the top moving surface is shown as a function of slip surface coverage
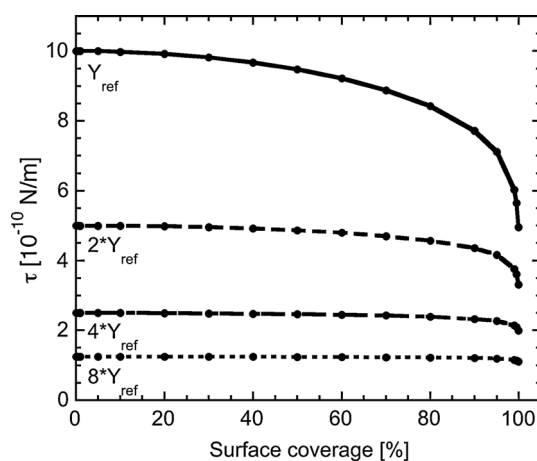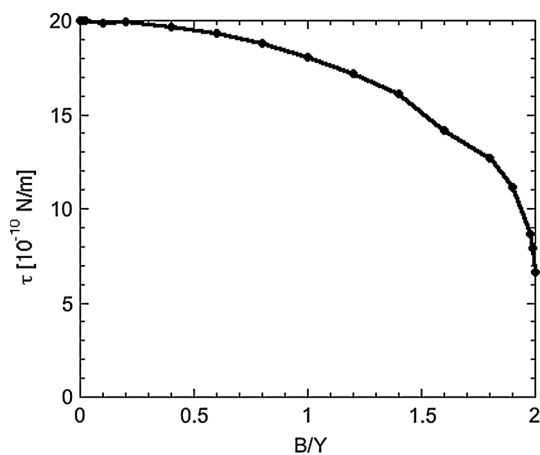

Fig. 5 The viscous stress of the reference system where $X = Y = 100$ nm, and a system when Y has been increased to $2 \times Y_{ref}$, $4 \times Y_{ref}$, and $8 \times Y_{ref}$ as a function of the slip surface coverage. The markers correspond to the simulated values, and the *line* is a guide for the eye

Fig. 6 The ratio of the size of the slip divided by the height, *B/Y*, shows that large effects on the viscous stress are visible when *B/Y* is close or above one. The markers correspond to the simulated values, and the *line* is a guide for the eye
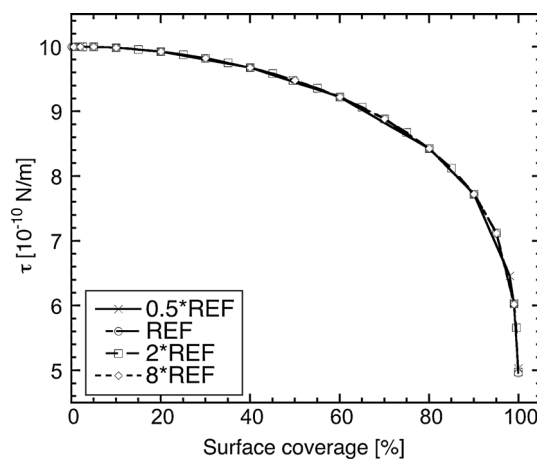

Fig. 8 The viscous stress for the reference system (REF) of 100×100 nm and systems $0.5 \times$ REF (50×50 nm), $2 \times$ REF (200×200 nm) and $8 \times$ REF (800×800 nm) show that the system to be scalable, i.e. applicable on all length scales. The markers correspond to simulated values, and the *line* is a guide for the eye
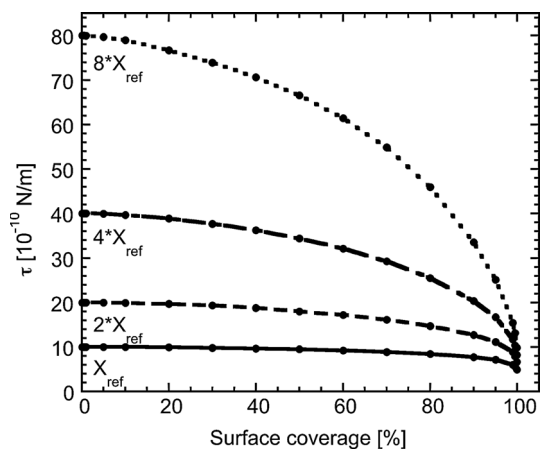

Fig. 7 The viscous stress for the reference system $X = Y = 100$ nm, and a system when X has been increased to $2 \times X_{ref}$, $4 \times X_{ref}$, and $8 \times X_{ref}$ versus the slip surface coverage. The markers correspond to the simulated values, and the *line* is a guide for the eye

coverage in Fig. 7. The results display that when the width X and the fraction of slip is increased, the viscous force on the top surface increases. For small slip fractions, an increase of X from 100 to 800 nm implies an increased viscous force by a factor of eight, whereas the increase is only doubled for large slips fractions. An increase of A times X gave a viscous stress A times that of X for small slip fractions (<1 %).

When the sides X and Y were varied the same amount simultaneously, the system is scalable (see Fig. 8). The latter statement proves that the results obtained in this study are valid on all length scales. Lauga and Stone (2003) have studied both transverse and longitudinal slip patterns in pipes and noticed a more significant flow rate for the transverse pattern than the longitudinal pattern. They also noticed that for small separation between slip patches, the
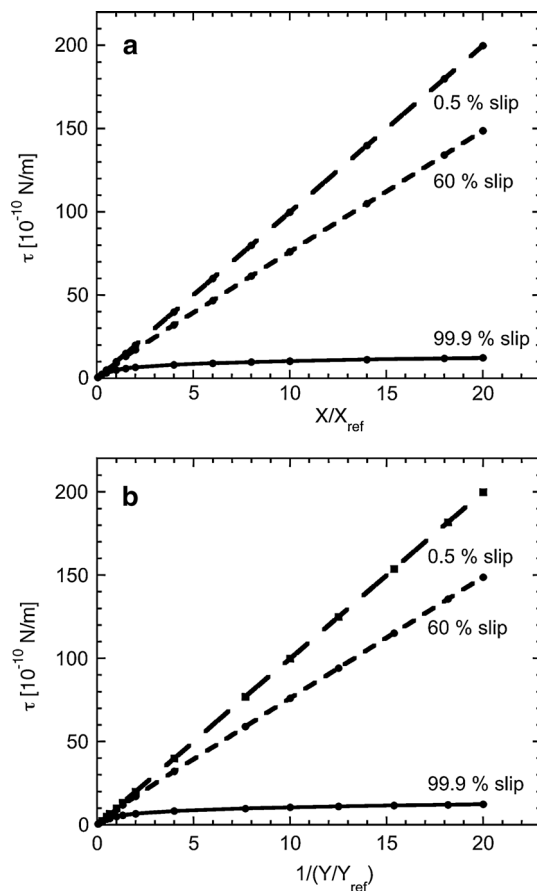

Fig. 9 The viscous stress on the top surface was determined for three different slip proportions on surface X, 0.5, 60 and 99.9 % slip for two cases. **a** $Y = 100$ nm and 5 nm $\leq X \leq 2,000$ nm, c.f. X_{ref} is 100 nm, and **b** $X = 100$ nm and 5 nm $\leq Y \leq 2,000$ nm, c.f. Y_{ref} is 100 nm. Markers correspond to simulated values, and the *line* is a guide for the eye

longitudinal slip patches result in an effective slip length a factor of two larger than the effective slip length obtained for the transverse slip patches.

To further investigate the behaviour of large slip fractions, the sides X and Y were normalized with respect to the reference system, X_{ref}, and Y_{ref} (100×100 nm). The viscous stresses are shown as functions of X/X_{ref} or $\frac{1}{Y/Y_{ref}}$. Model 1 was used and X and Y were varied between 5 and 2,000 nm. For comparison, the large slip fraction of X (99.9 %) was compared to a moderate (60 %) and a small (0.5 %) slip fraction. In Fig. 9, it is shown that small and moderate slip fractions show a linear dependence on the viscous stress whereas larger slip patches can be expressed by a logarithmic function.

The effect of the number of slip patches, keeping the total amount of slip constant, was studied by dividing the slip patch into several smaller patches (1–10). The slip patches were symmetrically distributed with adjacent no slip patches (Model system 3, size 100×100 nm). The slip proportion of X was varied from 10 to 99 %. The main results are that for small slip fractions, the viscous force on the top moving surface was not altered, independent of the number of slip patches (Fig. 10). However, when the slip fraction was increased, the number of slip patches had a profound effect on the viscous force. For a slip fraction of 99 %, the viscous force on the top moving surface decreased from 9.4×10^{-10} to 6.0×10^{-10} N/m, when dividing one patch into ten smaller patches, i.e. a decrease corresponding to 40 %. Generally, more pronounced effects on the viscous stress are displayed when the proportion of slip on the bottom surface is larger than 90 % and the number of slip patches is low (preferably only 1 slip patch). This is in agreement with Cottin-Bizonne et al. (2004) who have shown tha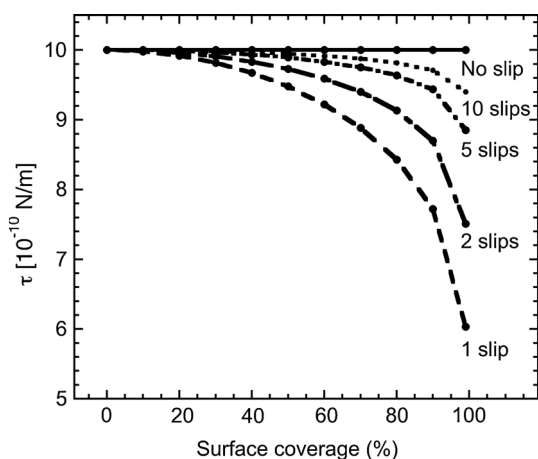t even a small proportion of no-slip surface in an otherwise slippery surface considerably decrease the effective slippage. The gas fraction in super-hydrophobic materials also affects slip, and it is shown that the slip length increases exponentially as the gas fraction approaches 100 %, both in experiments (Lee et al. 2008) and in computer simulations (Ybert et al. 2007; Samaha et al. 2011). Obviously, the stick patches adjacent to the slip regions act as effective barriers, slowing down the fluid velocity and preventing it to increase speed.

4 Conclusion

We have investigated fluid flow in a 2D model system in the nanometre range, with a central slip patch adjacent to two peripheral stick patches on the bottom surface X. The study has shown that the results are scalable, i.e. independent on length scale, and for a more pronounced effect of the fluid flow, the ratio of the size of the slip patch divided by the distances between the surfaces should be close or above one. For small slip fractions, an increase of X of A times gave rise to an A times increased viscous stress at the top surface, whereas an increase in the height Y implied an inverse relationship. For larger slip fractions, the relationship was logarithmic. When increasing the number of slip patches in the model, it was noticed that for smaller slip fractions, the number of slip patches did not have an impact on the viscous stress, whereas for larger slip fractions, a slip patch fragmentation resulting in several small slip patches showed minor effect on the viscous stress. To obtain a large effect on the viscous stress, the slip fraction should be large, preferably above 90 %, and the number of slip patches should be low, preferably one.

Fig. 10 The viscous stress compared to the slip surface coverage, showing the effect of the number and the proportion of slip patches. Results indicate that few and large slip patches have the largest effect on the viscous force

References

Bazant MZ, Vinogradova OI (2008) Tensorial hydrodynamic slip. J Fluid Mech 613:125–134

Bouzigues CI, Tabeling P, Bocquet L (2008) Nanofluidics in the Debye layer at hydrophilic and hydrophobic surfaces. Phys Rev Lett 101(11):114503

Brigo L, Natali M, Pierno M, Mammano F, Sada C, Fois G, Pozzato A, dal Zilio S, Tormen M, Mistura G (2008) Water slip and friction at a solid surface. J Phys Condens Matter 20(35):354016

Choi C-H, Westin KJA, Breuer KS (2003) Apparent slip flows in hydrophilic and hydrophobic microchannels. Phys Fluids 15(10):2897–2902

Cottin-Bizonne C, Barentin C, Charlaix É, Bocquet L, Barrat J (2004) Dynamics of simple liquids at heterogeneous surfaces: molecular-dynamics simulations and hydrodynamic description. Eur Phys J E Soft Matter Biol Phys 15(4):427–438

David Q (2005) Non-sticking drops. Rep Prog Phys 68(11):2495

Feuillebois F, Bazant MZ, Vinogradova OI (2010) Transverse flow in thin superhydrophobic channels. Phys Rev E 82(5):055301

Ishida N, Inoue T, Miyahara M, Higashitani K (2000) Nano bubbles on a hydrophobic surface in water observed by tapping-mode atomic force microscopy. Langmuir 16(16):6377–6380

Lauga E, Stone HA (2003) Effective slip in pressure-driven Stokes flow. J Fluid Mech 489:55–77

Lee C, Kim C-JC (2009) Maximizing the giant liquid slip on superhydrophobic microstructures by nanostructuring their sidewalls. Langmuir 25(21):12812–12818

Lee C, Choi C-H, Kim C-JC (2008) Structured surfaces for a giant liquid slip. Phys Rev Lett 101(6):064501

Pit R, Hervet H, Léger L (2000) Direct experimental evidence of slip in hexadecane: solid interfaces. Phys Rev Lett 85(5):980–983

Samaha MA, Tafreshi HV, Gad-el-Hak M (2011) Modeling drag reduction and meniscus stability of superhydrophobic surfaces comprised of random roughness. Phys Fluids 23(1):012001–012008

Stone HA, Stroock AD, Ajdari A (2004) Engineering flows in small devices: microfluidics toward a lab-on-a-chip. Annu Rev Fluid Mech 36:381–411

Stroock AD, Dertinger SK, Whitesides GM, Ajdari A (2002) Patterning flows using grooved surfaces. Anal Chem 74(20): 5306–5312

Tretheway DC, Meinhart CD (2002) Examination of the slip boundary condition by μ-PIV and lattice Boltzmann simulation. Phys Fluids 14(3):L9–L12

Tretheway DC, Meinhart CD (2004) A generating mechanism for apparent fluid slip in hydrophobic microchannels. Phys Fluids 16(5):1509–1515

Tyrrell JWG, Attard P (2001) Images of nanobubbles on hydrophobic surfaces and their interactions. Phys Rev Lett 87(17):176104

Wang CY (2003) Flow over a surface with parallel grooves. Phys Fluids 15(5):1114–1121

Whitesides GM (2006) The origins and the future of microfluidics. Nature 442(7101):368–373

Whitesides GM, Stroock AD (2001) Flexible methods for microfluidics. Phys Today 54(6):42–48

Ybert C, Barentin C, Cottin-Bizonne C, Joseph P, Bocquet L (2007) Achieving large slip with superhydrophobic surfaces: scaling laws for generic geometries. Phys Fluids 19(12):123601–123610

Zhou J, Belyaev AV, Schmid F, Vinogradova OI (2012) Anisotropic flow in striped superhydrophobic channels. J Chem Phys 136(19):194706–194711